



Membrane fouling behavior and microbial community succession in a submerged membrane bioreactor treating harbor oily wastewater*

Yan-jie WEI[†], Guo-yi LI

(Key Laboratory of Environmental Protection in Water Transport Engineering,
Tianjin Research Institute for Water Transport Engineering, Tianjin 300456, China)

[†]E-mail: wei_yj@126.com

Received Oct. 29, 2015; Revision accepted July 17, 2016; Crosschecked Aug. 18, 2016

Abstract: A membrane bioreactor (MBR) was established for treating harbor oily wastewater. It showed good removal performance for chemical oxygen demand (COD), oil content, suspended solids (SS), and other pollutants. However, serious membrane fouling occurred. It was recognized that the extracellular polymeric substances (EPS) accumulated on the membrane surface, especially the proteins, were of great importance for the transmembrane pressure (TMP) increment and membrane fouling. The MBR was optimized via improving aeration rate and reducing the ratio of A_r/A_d (A_r and A_d are the cross-sectional areas of the riser and the downcomer of the MBR). The increasing rate of TMP was slowed, indicating that the optimization strategy could effectively mitigate membrane fouling. Microbial community evolution was monitored and analyzed by polymerase chain reaction-denaturing gradient gel electrophoresis (PCR-DGGE), cloning, and sequencing of 16S ribosomal ribonucleic acid (rRNA) fragments. Results revealed that low community shift occurred during the whole operational period. *Geobacter* sp. and *Rhodocyclales* sp., which have also been identified by other studies in a petroleum refinery wastewater MBR or an infiltration basin receiving highway runoff, dominated in the MBR system throughout. *Comamonas* sp. was thought to accommodate the lower aeration rate in this study, while *Rhodocyclales* sp. preferred the higher aeration rate. In addition, during the operational time under high organic loading rate, a few species were present in abundance, and may have been responsible for the good removal performance at this time.

Key words: Membrane bioreactor (MBR) fouling, Extracellular polymeric substances (EPS), Harbor oily wastewater, Microbial community

<http://dx.doi.org/10.1631/jzus.A1500289>

CLC number: X52

1 Introduction

A membrane bioreactor (MBR) is able to provide a small footprint, perfect effluent, high biodegradation efficiency, and little excess sludge (Xia *et al.*, 2010). Thus, this technology has attracted increased interest and been widely applied in wastewater treatment and reuse. However, inevitable

membrane fouling, consequently leading to a decline in membrane permeability and an increase in operational cost, is still the major obstacle that hampers further development of MBR technology.

Extensive research has been carried out to better understand the fouling mechanism. It has been generally accepted that the membrane fouling is due to particle deposition on membrane surface and/or colloidal particle deposition inside membrane pores (Cosenza *et al.*, 2013). These processes are mainly affected by membrane materials, feedwater characteristics, sludge characteristics, and operating conditions (Judd, 2004; Meng *et al.*, 2009; Kim *et al.*, 2010; Cosenza *et al.*, 2013; Mannina and Cosenza, 2013;

* Project supported by the Science and Technology Project of the Ministry of Transport (No. 2011-329-224-330) and the National Nonprofit Institute Research Grants of Tianjin Research Institute for Water Transport Engineering (Nos. TKS100216, TKS130206, and TKS160215), China

 ORCID: Yan-jie WEI, <http://orcid.org/0000-0002-9007-450X>

© Zhejiang University and Springer-Verlag Berlin Heidelberg 2016

Estrada-Arriaga, *et al.*, 2015). Among them, sludge characteristics are considered to be directly affected by the feedwater characteristics and operating conditions (i.e., aeration, hydraulic conditions, sludge retention time (SRT), hydraulic retention time (HRT), organic loading rate, and food microorganism ratio (F/M)). Thus, it is assumed that sludge characteristics, including viscosity, mixed liquor suspended solids (MLSS) concentration, amount of filamentous bacteria, extracellular polymeric substances (EPS), and soluble microbial products (SMP), serve as the vital causes for membrane fouling. More specifically, it is believed that the EPS may have a primary role in membrane fouling (Cosenza *et al.*, 2013). However, due to the complexity of MBR systems and various wastewaters to be treated, the complex relationship of those fouling factors is still not clear. For some wastewater, a detailed understanding on how and which part of EPS has more significant influence on membrane fouling is still lacking (Delrue *et al.*, 2011; Cosenza *et al.*, 2013; Di Bella *et al.*, 2015). A better elucidation, clarifying the key fouling factors, will help in defining the optimum approach to mitigate membrane fouling in an MBR system.

Bacteria are key players in biological wastewater treatments (WWTs), and thus a firm knowledge of the bacterial population dynamics is crucial to understand environmental/operational factors affecting the efficiency and stability of the biological depuration process (Reboleiro-Rivas *et al.*, 2016). In recent years, DNA-based molecular techniques, like denaturing gradient gel electrophoresis (DGGE) of polymerase chain reaction (PCR) amplified 16S ribosomal ribonucleic acid (rRNA) gene fragments, offer a valuable tool for the characterization of the bacterial population diversity in biological wastewater treatment systems (LaPara *et al.*, 2002; Li A.J. *et al.*, 2008; Wei *et al.*, 2012). These techniques have been used to characterize the dynamics of microbial evolution in various wastewater treatment reactors (Li *et al.*, 2010; Zhang *et al.*, 2010; Aydin *et al.*, 2015). The molecular techniques are also applied in the MBR system to study the bacterial community structures. With the PCR-DGGE technique, Xia *et al.* (2010) investigated the effect of organic loading on the bacterial community composition of membrane biofilms in a submerged polyvinyl chloride MBR. Ziembinska *et al.* (2012) monitored the ammonia-oxidizing bacterial (AOB) communities in three MBRs for two months,

and found that landfill leachate can be effectively treated in an MBR with a higher sludge age for longer periods of time, and that this improvement in performance was correlated with an increase in AOB biodiversity. Tan *et al.* (2015) reported that the bacterial community in an MBR showed robust performance over ZnO nanoparticles exposure.

In this study, an MBR system was established for harbor oily wastewater treatment, owing to the higher biomass concentration retained by membrane filtration and longer SRT. A possible relationship between fouling and EPS was evaluated by means of scanning electron microscope (SEM) images, energy dispersive X-ray (EDX) analysis and Fourier transform infrared spectroscopy (FTIR) spectra, as well as qualitative analysis. The content and composition of EPS were also examined when the MBR system was optimized according to a model proposed by Chisti and Moo-Young (1993) and Li *et al.* (2000), so as to further verify the role of EPS in membrane fouling and the function of the optimization strategy. The microbial population dynamic during the whole operation period was monitored, to determine what kinds of bacteria are responsible for the pollutant removal performance and membrane fouling during long-term operation.

2 Materials and methods

2.1 Experimental set-up

Fig. 1 shows the schematic diagram of the experiment. A pilot-scale anoxic/oxic-MBR (A/O-MBR) with 500 L working volume was used. Two hollow flat-plate polyvinylidene fluoride (PVDF) fiber membrane modules (Motian, China) were submerged in the oxic zone. The nominal pore size of the membrane module was 0.2 μm , and the filtration area of each module was 1 m^2 . The MBR was operated at a constant permeate flux of 10 $\text{L}/(\text{m}^2 \cdot \text{h})$. The feed pump and suction pump were controlled by computer, and an intermittent suction effluent mode of 8 min-on/2 min-off was applied. Fine air bubbles were continuously supplied for aeration through microporous air diffusers at the bottom of the oxic zone. The air flow rate was controlled by a rotermeter, with an air flow rate of 0.1–1.0 m^3/h . The membrane module did not experience hydrodynamic and chemical cleaning before the end of the experiment.

Floc-like sludge from an oxidation ditch of a local harbor oily wastewater treatment plant was added to the MBR as inocula, resulting in an initial MLSS of 5.0 g/L. The SRT was maintained at 50 d.

The system was fed with real harbor oily wastewater coming from a local harbor oily wastewater treatment plant in Tianjin Harbor, China. Influent of A/O-MBR had been pre-treated by coagulation-sedimentation. Composition of the influent fed to the reactor is summarized in Table 1.

2.2 Operational strategy

It is known that the improvement of the hydrodynamic condition in MBR systems, including cross-flow velocity (CFV) along the membrane surface, can effectively mitigate membrane fouling (Bacchin and Espinasse, 2005). For this purpose, CFV was usually kept around 1 m/s in MBRs treating municipal wastewater (Li J. *et al.*, 2008). Therefore, it could be inferred that for a sufficiently long membrane life, a higher CFV should be obtained in MBRs treating oily wastewater.

The CFV of the submerged MBR was equated with the liquid circulation velocity U_{Lr} , which could

be calculated following the procedure reported by Chisti and Moo-Young (1993) and Li *et al.* (2000):

$$U_{Lr} = \left[\frac{2gh_D(\varepsilon_r - \varepsilon_d)}{K_B \left(\frac{A_r}{A_d} \right)^2 \frac{1}{(1 - \varepsilon_d)^2}} \right]^{0.5}, \quad (1)$$

where U_{Lr} is the superficial liquid velocity in the riser of MBR, m/s; g is the gravitational acceleration, m^2/s ; h_D is the gas-liquid dispersion height in the MBR, m; A_r and A_d are the cross-sectional areas of the riser and the downcomer, respectively, m^2 ; ε_r and ε_d are the fractional-gas-holdup values of the riser and the downcomer, respectively; K_B is the frictional-loss coefficient for the bottom zones.

It could be seen that a higher aeration rate and a lower ratio of A_r/A_d are in favor of higher superficial liquid velocity in the riser of MBR, or CFV. However, the higher aeration rate would also result in higher operational costs, and the lower ratio of A_r/A_d would lead to larger floor area. Thus, proper parameters should be optimized.

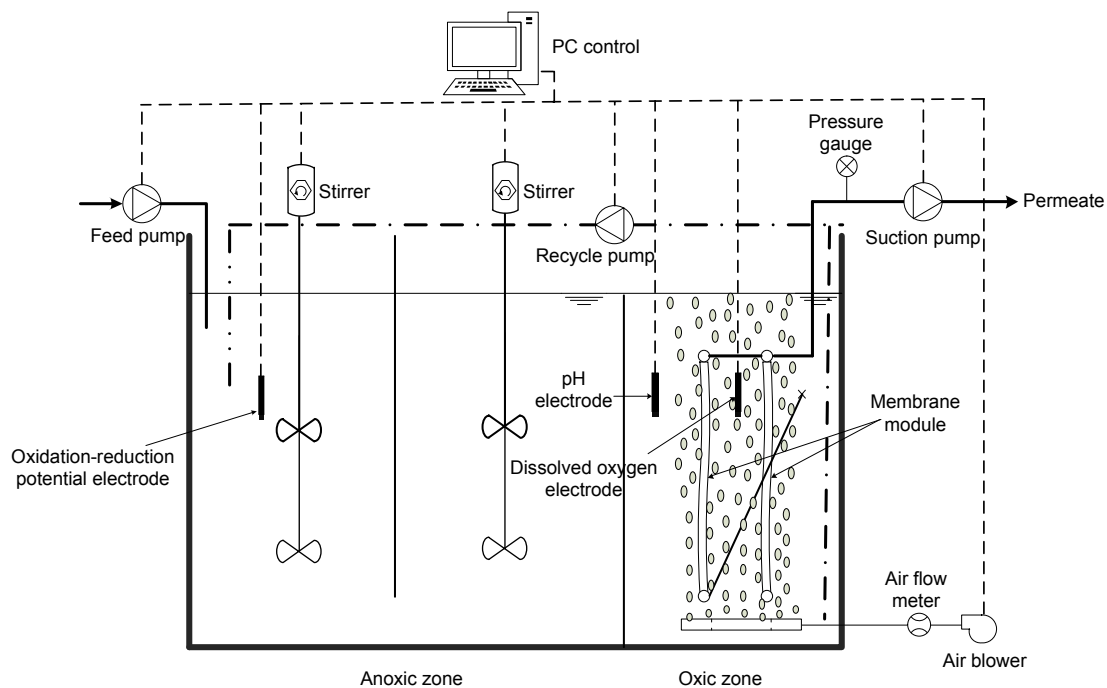


Fig. 1 Schematic diagram of the pilot-scale A/O-MBR

Two hollow flat-plate PVDF fiber membrane modules were submerged in the oxic zone

Table 1 Characteristics of feed and effluent from different zone

Item	Feed	Effluent of anoxic zone	Effluent of MBR
COD (mg O ₂ /L)	732.7 ±262.9	427.6 ±155.6	48.1 ±31.4
Oil content (mg/L)	48.2 ±13.1	8.8±6.3	–
Monocyclic aromatic hydrocarbons			
Benzene* (µg/L)	251	172	16
Toluene* (µg/L)	490	332	37
Ethylbenzene* (µg/L)	80	23	–
Meta & para-xylene (µg/L)	566	352	71
Ortho-xylene (µg/L)	411	233	42
Styrene (µg/L)	25	17	–
Isopropylbenzene (µg/L)	22	10	–
n-Propylbenzene (µg/L)	10	13	–
1,3,5-Trimethylbenzene (µg/L)	117	68	–
1,2,4-Trimethylbenzene* (µg/L)	297	179	–
Sec-butylbenzene (µg/L)	17	7	–
p-Isopropyltoluene (µg/L)	17	5	–
Polynuclear aromatic hydrocarbons			
Naphthalene* (µg/L)	447	186	29
2-Methylnaphthalene (µg/L)	791	233	63
Acenaphthylene* (µg/L)	55	26	–
Phenanthrene* (µg/L)	305	133	16
Pyrene* (µg/L)	57	28	6
Benzo(a)anthracene* (µg/L)	19	5	–
Chrysene* (µg/L)	115	48	6
pH	7.71	7.56	8.01
Suspended solids (SS) (mg/L)	195.6	31	–
Cl ⁻ (mg/L)	3532	3765	4033
Cu* (×10 ⁴ µg/L)	5.11	1.03	0.062
Zn* (µg/L)	52.5	30.1	2.6
As* (µg/L)	31.5	21.6	8.9
Sb* (µg/L)	10.0	8.2	0.4
Se* (µg/L)	11.2	5.3	1.8
Cr* (µg/L)	17.4	4.7	1.6
Ni* (µg/L)	12.8	3.8	0.7
Pb* (µg/L)	8.8	5.2	–
Hg* (µg/L)	6.5	1.6	0.3

* In the list of priority pollutants of United States Environmental Protection Agency (USEPA); –: not detected or less than the limit of report values

The experiment lasted for 320 d in total, including the first stage, suspended stage, and second stage. During the first stage, the aeration rate of the MBR was fixed at 0.40 m³/h, and the ratio of A_r/A_d was 0.21, with a CFV of 0.78 m/s. To gain a higher CFV to mitigate membrane fouling, both the aeration rate and A_r/A_d were optimized in the suspended stage according to the models proposed by Chisti and Moo-Young (1993) and Li *et al.* (2000). Eventually, the aeration rate of the MBR increased to 0.45 m³/h during the second stage. A_r/A_d decreased to 0.18, with a CFV of 1.13 m/s. Meanwhile, the membrane modules were replaced by new ones. Fresh floc-like sludge was added into the MBR, with the MLSS of 5 g/L, just as at the beginning of the first stage.

2.3 Analytical methods

COD, oil content, Cl⁻ content, SS, and MLSS were measured regularly according to the standard methods (APHA, 1998). pH was determined by a pH meter (Hanna HI9145, Italy). Heavy metal was analyzed by an inductively coupled plasma mass spectrometer (PerkinElmer SCIEX-ELAN DRC-e, USA) and a mercury vapourmeter (Milestone DMA80, Italy). Monocyclic aromatic hydrocarbons (MAH) were tested by a gas chromatography-mass spectrometer (Agilent 7890B-5977A, USA). Polynuclear aromatic hydrocarbons (PAH) were detected by a gas chromatography-mass spectrometer (Agilent 7890A/5975C, USA).

The morphology and structure of the membrane surface were observed using an environmental SEM (Phillips XL30, the Netherlands). EDX analysis was accomplished by an X-ray energy spectrometer (Genesis XM2, USA). A spot size of about 70 nm was used to record EDX spectra and stoichiometric ratios were calculated from atomic percentages given by EDX spectra. EDX calibration standards were run to obtain quantitative analyses of major elements on the membrane surface (Zhang *et al.*, 2008b). The deposition of biopolymers on the membrane surface was characterized by Fourier transform infrared spectroscopy (Nexus™, USA). Sludge morphology was observed under an optical microscope (HIROX KH-7700, USA). Specific resistance to filtration (SRF) of sludge was tested according the method described by Zhang (2000).

The EPS of the mixed liquor in the membrane reactor was extracted using the method described by Wang *et al.* (2010). The EPS of the cake layer attached to the membrane was extracted according the steps described by Zhang *et al.* (2008b). The polysaccharides content was determined by the phenol-sulfuric acid method (Gerhardt *et al.*, 1994). The protein content was determined by the revised Lowry method (Frølund *et al.*, 1996).

2.4 DNA extraction, PCR amplification, and DGGE

Activated sludge samples were collected from the MBR system. The sludge from approximately 8 mg of MLSS was transferred into a 1.5-ml Eppendorf tube and then centrifuged at 14000g for 10 min. The supernatant was then removed, and the pellet was stored at -70°C until further analysis (Zhang *et al.*, 2010).

Genomic DNA of the biomass in sludge and granule samples was extracted using an E.Z.N.A.TM Soil DNA Kit (OMEGA D5625-01, USA). Subsequently, the 16S rRNA gene was amplified by a nested PCR approach. After the first round of amplification, a nested PCR was performed on the PCR products with a second primer pair allowing the amplification of an internal fragment. These primers and PCR conditions are summarized in Table 2. All PCR amplicons were examined by electrophoresis in 1.5% (weight/volume) agarose with ethidium bromide staining to confirm the product size. PCR

amplification was performed with a GoTaq Master Mix (Promega, USA).

The PCR-amplified DNA products were separated by DGGE on polyacrylamide gels (8%, 37.5:1 acrylamide-bisacrylamide) with a linear gradient of 35%–55% denaturant (100% denaturant=7 mol/L urea plus 40% formamide). Gels were run for 7 h at 150 V in $1\times$ TAE buffer maintained at 60°C . Denaturing gradient gels were poured and run using the DGGE-2001 System (C.B.S. Scientific, Del Mar, USA). Gels were silver-stained, air dried, and scanned following the prescriptions described elsewhere (Sanguinetti *et al.*, 1994).

2.5 Cloning and sequencing analysis

Selected DGGE bands were excised and dissolved in 50 μl Milli-Q water overnight, at 4°C . DNA was recovered from the gel by freeze-thawing three times. Using the primer set F357/R518 without GC-clamp, 3 μl of these DNA band samples were reamplified by the same PCR procedure described previously. The PCR products were cloned using the PGEMTM-T Easy vector system (Promega, Madison, USA). The positive colonies were amplified with F357/R518. PCR amplicons were submitted for sequencing using ABI 3730 capillary sequencers (PE Applied Biosystems, Invitrogen, China) (Zhang *et al.*, 2010). Sequence data were analyzed in comparison with the 16S rRNA sequences in the GenBank by BLASTN search (National Centre for Biotechnology Information, USA) for species identification.

Table 2 Primer characteristics and conditions for nested PCR

PCR	Primer	Sequence	Reaction solution	PCR condition	Reference
1st round	R1378	5'-CGGTGTGTACAAG GCCCCGGAACG-3'	25 μl in 0.2-ml Axygen PCR tubes, containing 1.25 U of <i>Taq</i> DNA polymerase (Promega, China), 5 μl of $10\times$ buffer minus, 1.5 mmol/L MgCl_2 , 1 μl template DNA, 0.2 mmol/L dNTPs, and 0.2 $\mu\text{mol/L}$ of each primer	5 min at 94°C , followed by 30 cycles of 1 min at 94°C , 1 min at 65°C (-1°C each cycle and 20 cycles at 55°C), and 1 min at 72°C , followed by a 7-min final extension at 72°C	Tu <i>et al.</i> , 2012
	63F	5'-CAGGCCTAACACA TGCAAGTC-3'			
2nd round	GC-F338	5'-CGCCCCGCCGC GCGCGGCGGG CGGGGCGGGG GCACGGGGGG ACTCCTACGG GAGGCAGCAG-3'	50 μl in 0.2-ml Axygen PCR tubes. The reaction solution contained 2.5 U of <i>Taq</i> DNA polymerase (Promega, China), 5 μl of $10\times$ buffer minus, 2.0 mmol/L MgCl_2 , 2 μl template DNA (10–100 ng), 0.2 mmol/L dNTPs, and 0.25 $\mu\text{mol/L}$ of each primer	5 min at 95°C , followed by 30 cycles of 1 min at 94°C , 1 min at 65°C (-0.5°C each cycle and 10 cycles at 55°C), and 1 min at 72°C , followed by a 5-min final extension at 72°C	Muyzer <i>et al.</i> , 1993
	R518	5'-ATT ACC GCG GCT GCT GG-3'			

3 Results and discussion

3.1 MBR performance

Table 1 and Fig. 2 show the changes and removal efficiencies of main pollutants fed to the system. During the first stage, the organic loading rate (OLR) of the MBR was 0.72–1.25 kg COD/(m³·d). With the acclimatization of microorganisms to influent compounds, COD removal efficiency (RE) gradually increased and stabilized around 90% afterwards.

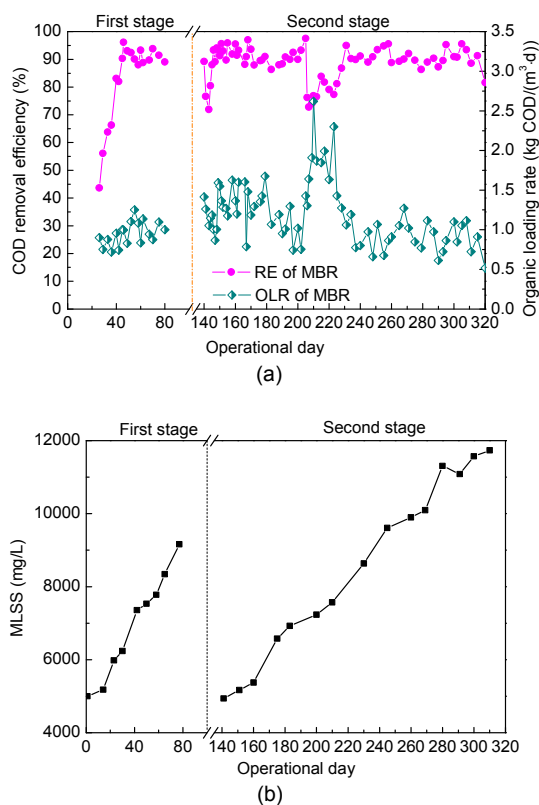


Fig. 2 Organic removal performance (a) and change of sludge concentration at different stages (b)

In the second stage, COD removal efficiency was still about 90%, except in the middle phase with higher shock load. During days 200–230, the OLR increased sharply to 1.63–2.62 kg COD/(m³·d) due to higher influent COD content. The COD removal efficiency decreased, but it resumed to a stable range of 88%–95% in a short period. When the influent COD was (427.6±155.6) mg/L, the effluent concentration was stationary at (48.1±31.4) mg/L.

There were a few pretreatment steps before the MBR for the oil removal but the influent oil content

of MBR was still as high as (8.8±6.3) mg/L. In light of the entrapment role of the membrane module, the bioreactor became a relatively closed system as far as the microbial metabolism was concerned (Wang *et al.*, 2008). Therefore, the oil content was not detected after the MBR treating.

The MBR also exhibited good removal performance for recalcitrant compounds (MAH and PAH), SS, and other elements in the list of priority pollutants of USEPA. Ammonium was not a major concern because the average influent concentration of the MBR system was fairly low.

Fig. 2b shows the changes of biomass concentration in the MBR. It increased from 5000 mg/L to 9159 mg/L during the first stage, and from 4939 mg/L to 11 730 mg/L in the second stage.

3.2 Membrane fouling behavior

Membrane fouling was usually monitored using transmembrane pressure (TMP) under constant flux mode. The evolution of permeate flux and TMP are depicted in Fig. 3. The flux was fixed at around 10 L/(m²·h) via a constant flow suction pump. The TMP increased sharply, and reached 30 kPa after 78 d.

Specific resistance to filtration (SRF) of sludge is widely used to foresee performances of full-scale filters and to compare the sludge behavior from different plants against filtration processes. It represents the resistance to filtration of a theoretical sludge panel having unitary weight in dry solids per unit of filtering surface (Pontoni *et al.*, 2015). The evolution of SRF in this study is shown in Fig. 3. It did not significantly change within 25 d. The rapid increase of SRF was completed between the 30th day and 70th day, and it was up to 4.18×10^{13} m/kg on the 70th day, meaning a higher aptitude of sludge to be dehydrated via filtration, and higher energy to be consumed for ensuring the constant flux (Mannina *et al.*, 2016b). In addition, the increase of SRF was closely associated with the TMP augmentation, suggesting that sludge characteristics would be the major pressure exerted on MBR fouling.

In general, membrane fouling is attributed to initial pore blocking followed by cake formation (Meng *et al.*, 2007). The sludge layer was thought to be the main cause of membrane fouling and the increment of transmembrane resistance (Mannina *et al.*, 2016a). The SEM images reveal the outer morphology of foul

membrane surface (Fig. 4). It can be seen that multiple sludges were tightly linked together by a cement-like substance forming a compact structure.

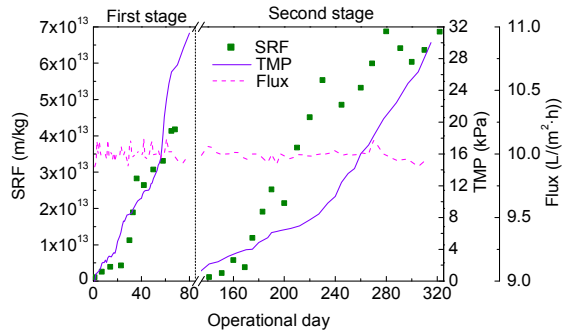


Fig. 3 Variations of TMP and flux of the MBR, as well as the SRF of the sludge

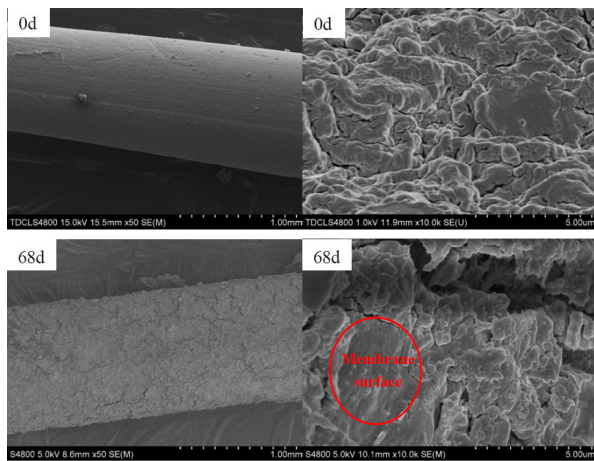


Fig. 4 SEM images of the original membrane and the membrane sample on the 68th day, showing the surfaces of clean and fouled membranes, respectively

EDX and FTIR analyses were performed to confirm the major components of the fouling layer (Figs. 5 and 6). In comparison with the original chemical composition, multi-valent metal elements, such as Zn, Mg, Al, and Ca, were detected. It was well known that EPS would be produced during the microbial metabolism, and prefers to bind multi-valent metals due to the formation of stable complexes (Rudd et al., 1984).

Additionally, the spectrum showed peaks mainly between 3500 cm^{-1} and 600 cm^{-1} . The broad peak at 3284.25 cm^{-1} is due to the stretching vibration of the O–H bond in hydroxyl functional groups, and the sharp peak at 2921.17 cm^{-1} is due to stretching of C–H bond (Meng et al., 2007). The peak at

1632.63 cm^{-1} is sensitive to C=O stretching vibration of the protein amide I. The peak at 1543.72 cm^{-1} is assigned to the out-of-phase combination of the NH in-plane bend and the CN stretching vibration of the protein amide II (Barth and Zscherp, 2002). The peaks in the spectral range from 1250 cm^{-1} to 1000 cm^{-1} are due to the contribution of nucleic acid phosphodiester groups and phospholipids, as well as to the C–O absorption of carbohydrates (Ami et al., 2014). In Fig. 6 the FTIR spectra of membrane foulants show that the major components of the foulants included proteins and polysaccharide materials. Proteins and carbohydrates are the dominant components typically found in EPS.

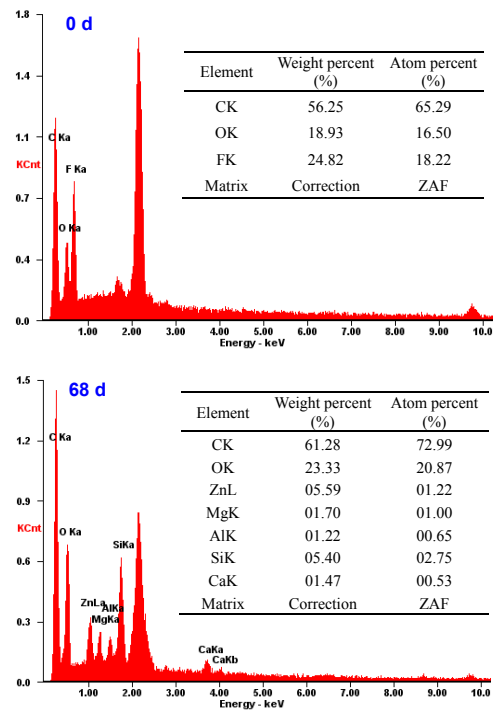


Fig. 5 Elemental analysis of the original membrane and cake layer on the 68th day

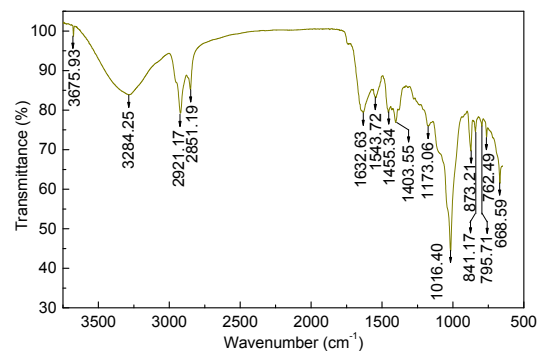


Fig. 6 FTIR spectra of the cake layer on the 68th day

Taken together with the analysis above, it could be inferred that EPS would be the major component of the fouling layer, and a probable index for membrane fouling.

3.3 Relationship between EPS content and membrane fouling behavior

The qualitative composition of the EPS was determined to investigate the deposition behavior of EPS on the membrane surface, and further membrane fouling, so as to get further insights into the assumed relationship between EPS and membrane fouling behavior. Fig. 7 shows the EPS composition of the mixed liquor in the membrane reactor. The original concentrations of proteins (PN) and polysaccharides (PS) were 31.9 mg/g VSS and 7.9 mg/g VSS, respectively. The polysaccharides concentration did not show significant change subsequently, and stabilized at 9.2–11.0 mg/g VSS. Rapid increase of proteins concentration had occurred, and it reached around 98.5 mg/g VSS on the 58th day. The concentration ratio of PN/PS showed similar trends to that of protein concentration.

Taken in conjunction with the data shown in Figs. 3 and 7, it can be observed that protein concentration of mixed liquor was dramatically related to SRF. The exponential relationship is illustrated in Fig. 8 by a positive correlation coefficient of 0.934 (data of the second stage were used here, and would be discussed later). These results clearly implied that proteins, the major component of EPS of the mixed liquor, would stimulate the increase of sludge SRF in a very significant way.

The EPS composition of the cake layer attached to the membrane is depicted in Fig. 9. On the 42nd day, the concentrations of proteins and polysaccharides were 133.9 mg/g VSS and 38.1 mg/g VSS, respectively. These parameters increased to 157.4 mg/g VSS and 49.6 mg/g VSS on the 65th day, implying that the EPS had significantly accumulated on the membrane surface.

Based on the above discussion, it could be inferred that the EPS of the mixed liquor or accumulated on the membrane surface (mainly the proteins) were of great importance for increase of sludge SRF and TMP, and consequent membrane fouling. But which one played the effective trigger for membrane fouling still needs to be fully understood.

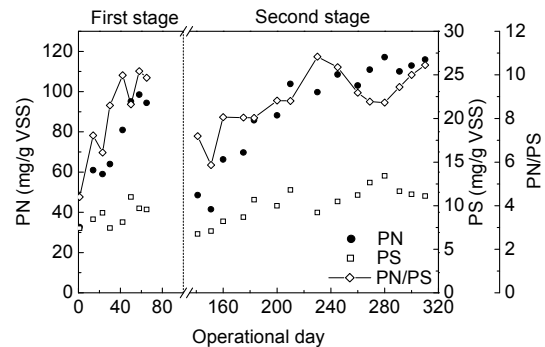


Fig. 7 EPS composition of the mixed liquor in the membrane reactor, showing the changes of the concentrations of PN and PS, and the concentration ratio of PN/PS

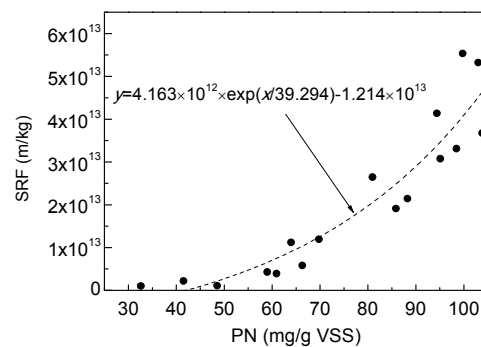


Fig. 8 Proportional relationship between the concentrations of proteins and SRF

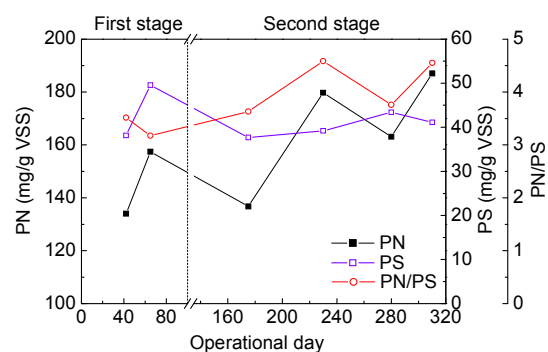


Fig. 9 EPS composition of the cake layer in the membrane reactor, showing the changes of the concentrations of PN and PS, and the concentration ratio of PN/PS

3.4 Optimization of the MBR system

To achieve a longer membrane life, many manufacturers of hollow fiber membrane have made strict user notes that influent oil content (in terms of N-Hexane Extract, N-HEX) should be eliminated to a level of below 3 mg/L (MOTIMO, 2006). As a matter

of fact, the influent oil content of the MBR was as high as (8.8 ± 6.3) mg/L in this study, which would aggravate the fouling step, as demonstrated by the sharp increment of TMP in Fig. 3. To weaken the effect of oil pollutant on membrane fouling, the MBR was optimized by way of increasing aeration rate and reducing A_p/A_d . The CFV increased from 0.78 m/s to 1.13 m/s. As a result, the TMP of the MBR system still increased, but slowly. The change in TMP from 0.35 kPa to 30 kPa took about 180 d (Fig. 3), over twice the time taken before the operation optimization (75 d), indicating that the optimization could effectively reduce the rate of transmembrane pressure under constant flux mode, and significantly mitigate membrane fouling.

The deposition behaviors of EPS of the mixed liquor and SRF change after adjustment are illustrated in Figs. 3 and 7. In comparison with the situation in the first stage, the increasing rate of protein content and SRF was the same, or even higher, meaning that the optimization exerted no or positive effect on EPS secretion of the mixed liquor and sludge SRF in the MBR system. This was inconsistent with the fouling behavior.

The deposition behaviors of EPS accumulated on the membrane surface exposed to the adjustment are shown in Fig. 9. Protein content increased slowly, implying that the optimization played a crucial role in slowing down the increasing rate of EPS content (mainly the proteins content) of the fouling layer. This phenomenon could explain why the CFV was improved after optimization, because EPS can be removed by the shear stress of fluid mechanics on the membrane surfaces (Ying *et al.*, 2010).

A solid conclusion can be drawn that the EPS which accumulated on the membrane surface, especially the proteins, were of great importance for the TMP increment and membrane fouling.

3.5 Microbial population dynamics at different operational stages

Bacterial community DNA was extracted from the sludge, which was sampled once every few days. Using the DNA obtained from DNA Kit method as template, 250-bp fragments of the V3 hypervariable region of the 16S rRNA gene were obtained as expected. DGGE was carried out to determine the genetic fingerprint of these PCR amplification products,

and the profiles are illustrated in Fig. 10. From the similarity diagram and cluster analysis by unweighted pair group method (UPGMA), it is noticeable that low community shift occurred during the whole operational period, and marginal changes of DGGE bands and patterns were observed at different operational stages. It can be seen that several dominant bands appeared across all biomass samples. This indicates that the species represented by these bands were predominant populations throughout the experiment.

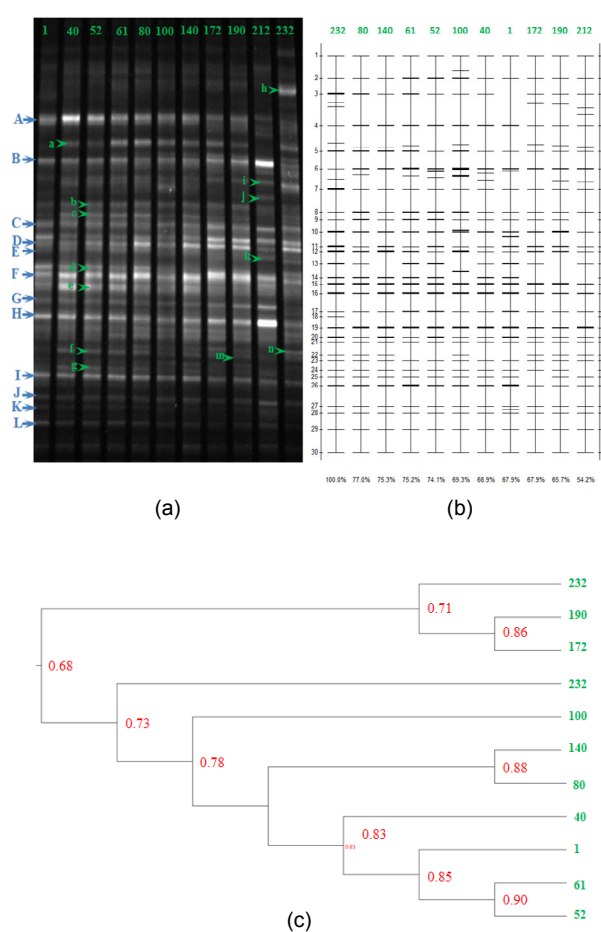


Fig. 10 DGGE profiles of the bacterial communities in the MBR at different operational stages

(a) DGGE profile (the predominant bands are labeled A–L, and bands a–n are dynamic species existing in partial samples); (b) Similarity diagram of sample lanes (DGGE pattern of day 232 is defined as 100%, and values along the bottom indicate the similarity coefficient with day 232); (c) Cluster analysis of DGGE by UPGMA (values in the cluster indicate the similarity coefficient with each other). Lane labels along the top or right side show sampling time (in days) from startup of the bioreactor

There were also some relatively persistent species, like band_A, which were very intense during the first stage with low aeration rate, but became depleted or not detectable during the second stage with higher aeration rate. This phenomenon indicates that the population represented by band_A accommodated the low aeration rate. Conversely, some species, like band_D, band_E, and band_F, were very intense in the sludge samples at the second stage, indicating that these species may prefer the higher aeration rate. In addition, species marked by band_B and band_H were particularly intense in lane 212. Taken together, the results shown in Fig. 3 and Table 2 suggest that the corresponding species may metabolically respond to high OLR.

3.6 Sequencing results and analysis

Nine bands were carefully excised, amplified, and sequenced to identify microbial species, and the nucleotide sequences were compared with previously identified 16S rRNA gene sequences in the GenBank database using BLASTN. The results are shown in Table 3. It can be seen that band_A was most closely related to uncultured *Comamonadaceae bacterium* clone PII8C, which was identified in a petroleum refinery wastewater membrane bioreactor fed with a

high phenolic load (Silva *et al.*, 2010). Previous studies reported that dominant microbial species of the membrane cake layer contained *Comamonadaceae* (Gao and Xin, 2014). *Comamonas* sp. would excrete an amount of slime-EPS and capsular-EPS, and result in severe fouling (Zhang *et al.*, 2008a). These findings were identical to the results in this study. Band_A, representing *Comamonadaceae*, was intense in the sludge samples under serious membrane fouling, and died away during the second stage after operation optimization, further implying that the optimization could efficiently slow down the membrane fouling process.

Band_C was closely related to uncultured sludge bacterium clone ASB54, which was thought of as being one isolated lipolytic gene from activated sludge (Liaw *et al.*, 2010). Band_D and Band_F had high homologies in the nucleotide sequence with uncultured *Geobacteraceae bacterium* clone PM5_7.0-02, which was isolated from an infiltration basin receiving highway runoff (Rotaru *et al.*, 2012). Band_L was closely related to uncultured *Rhodocyclaceae bacterium* clone PM5_-0.3-05, which was also detected in the infiltration basin receiving highway runoff (Rotaru *et al.*, 2012). Band_c was most closely related to *Hydrogenophaga* sp.

Table 3 Sequence analysis and species identification of selected DGGE bands for the sludge samples

Band	Accession	Description	Coverage ratio (%)	Identity (%)
A	FJ439084.1	Uncultured <i>Comamonadaceae bacterium</i> clone PII8C 16S rRNA gene, partial sequence	97	100
C	FJ947138.1	Uncultured sludge bacterium clone ASB54 16S rRNA gene, partial sequence	100	99
D	JQ177533.1	Uncultured <i>Geobacteraceae bacterium</i> clone PM5_7.0-02 16S rRNA gene, partial sequence	99	98
E	HQ484708.1	Uncultured bacterium clone Pohang_WWTP_February.2006_1486 16S rRNA gene, partial sequence	99	99
F	JQ177533.1	Uncultured <i>Geobacteraceae bacterium</i> clone PM5_7.0-02 16S rRNA gene, partial sequence	100	99
L	JQ177848.1	Uncultured <i>Rhodocyclaceae bacterium</i> clone PM5_-0.3-05 16S rRNA gene, partial sequence	97	96
c	JQ522966.1	<i>Hydrogenophaga</i> sp. A11(2012) 16S rRNA gene, partial sequence	100	98
d	JQ793317.1	Uncultured <i>Thiobacillus</i> sp. clone BWET3cm33 16S rRNA, partial sequence	100	99
e	JQ624351.1	Uncultured <i>beta proteobacterium</i> clone OTU-24-40m.ABB 16S rRNA gene, partial sequence	100	100

4 Conclusions

1. An A/O-MBR was used to treat harbor oily wastewater. It revealed good removal performances for COD, oil content, monocyclic aromatic hydrocarbons, polynuclear aromatic hydrocarbons, SS, and other elements in the list of priority pollutants of USEPA. However, serious membrane fouling occurred when the TMP increased to 30 kPa under constant flux mode in a short time.

2. It is reasonable to consider that the EPS content would be a probable index for membrane fouling by means of SEM images, EDX analysis, and FTIR spectra. The qualitative analysis further verified that the EPS accumulated on the membrane surface, especially the proteins, were of great importance for the TMP increment and membrane fouling.

3. The MBR was optimized by way of increasing aeration rate and reducing A_r/A_d . The evolution of TMP in the MBR system, and the deposition behavior of EPS substantiated that the optimization strategy could effectively reduce the rate of TMP under constant flux mode, and significantly mitigate membrane fouling.

4. Results of PCR-DGGE indicated that low community shift occurred during the whole operational period. The species marked by band_A accommodated the low aeration rate, and were predominant during the first stage, and may metabolically respond to severe fouling. Some species, like band_D, band_E, and band_F, preferred the higher aeration rate, and were very intense in the sludge samples at the second stage. Species marked by band_B and band_H may metabolically respond to high OLR.

5. Sequencing analysis demonstrated that some dominant species were also identified by other researchers in a petroleum refinery wastewater membrane bioreactor, or an infiltration basin receiving highway runoff.

References

Ami, D., Posterl, R., Mereghetti, P., et al., 2014. Fourier transform infrared spectroscopy as a method to study lipid accumulation in oleaginous yeasts. *Biotechnology for Biofuels*, **7**(1):12.
<http://dx.doi.org/10.1186/1754-6834-7-12>

APHA (American Public Health Association), 1998. Standard Methods for the Examination of Water and Wastewater,

20th Edition. APHA, Washington DC, USA.

Aydin, S., Shahi, A., Ozbayram, E.G., et al., 2015. Use of PCR-DGGE based molecular methods to assessment of microbial diversity during anaerobic treatment of antibiotic combinations. *Bioresource Technology*, **192**:735-740.
<http://dx.doi.org/10.1016/j.biortech.2015.05.086>

Bacchin, P., Espinasse, B., 2005. Distributions of critical flux: modeling, experimental analysis and consequences for cross-flow membrane filtration. *Journal of Membrane Science*, **250**(1-2):223-234.
<http://dx.doi.org/10.1016/j.memsci.2004.10.033>

Barth, A., Zscherp, C., 2002. What vibrations tell us about proteins. *Quarterly Reviews of Biophysics*, **35**(4):369-430.
<http://dx.doi.org/10.1017/S0033583502003815>

Chisti, Y., Moo-Young, M., 1993. Improve the performance of airlift reactors. *Chemical Engineering Process*, **6**:38-45.

Cosenza, A., Di Bella, G., Mannina, G., et al., 2013. The role of EPS in fouling and foaming phenomena for a membrane bioreactor. *Bioresource Technology*, **147**:184-192.
<http://dx.doi.org/10.1016/j.biortech.2013.08.026>

Delrue, F., Stricker, A.E., Mietton-Peuchot, M., et al., 2011. Relationships between mixed liquor properties, operating conditions and fouling on two fullscale MBR plants. *Desalination*, **272**(1-3):9-19.
<http://dx.doi.org/10.1016/j.desal.2010.12.056>

Di Bella, G., Di Prima, N., Di Trapani, D., et al., 2015. Performance of membrane bioreactor (MBR) systems for the treatment of shipboard slops: assessment of hydrocarbon biodegradation and biomass activity under salinity variation. *Journal of Hazardous Materials*, **300**:765-778.
<http://dx.doi.org/10.1016/j.jhazmat.2015.08.021>

Estrada-Arriaga, E.B., Nacheva, P.M., García-Sánchez, L., 2015. Effect of mixed liquor volatile suspended solids on membrane fouling during short and long-term operation of membrane bioreactor. *Ingeniería y Ciencia*, **11**(21):137-155.
<http://dx.doi.org/10.17230/ingciencia.11.21.7>

Frolund, B., Palmgren, R., Keiding, K., et al., 1996. Extraction of extracellular polymers from activated sludge using a cation exchange resin. *Water Research*, **30**(8):1749-1758.
[http://dx.doi.org/10.1016/0043-1354\(95\)00323-1](http://dx.doi.org/10.1016/0043-1354(95)00323-1)

Gao, D.W., Xin, X.D., 2014. Analysis of microbial community structure and metabolites during the MBR membrane fouling process. *Journal of Harbin Institute of Technology*, **46**(2):26-32 (in Chinese).

Gerhardt, P., Murray, R.G.E., Wood, W.A., et al., 1994. Methods for General and Molecular Bacteriology. American Society for Microbiology, Washington DC, USA, p.518.

Judd, S., 2004. A review of fouling of membrane bioreactors in sewage treatment. *Water Science Technology*, **49**(2):229-235.

Kim, H.G., Jang, H.N., Kim, H.M., et al., 2010. Effects of the sludge reduction system in MBR on the membrane permeability. *Desalination*, **250**(2):601-604.
<http://dx.doi.org/10.1016/j.desal.2009.09.032>

- LaPara, T.M., Nakatsu, C.H., Pantea, L.M., et al., 2002. Stability of the bacterial communities supported by a severn-stage biological process treating pharmaceutical wastewater as revealed by PCR-DGGE. *Water Research*, **36**(3):638-646.
[http://dx.doi.org/10.1016/S0043-1354\(01\)00277-9](http://dx.doi.org/10.1016/S0043-1354(01)00277-9)
- Li, A.J., Yang, S.F., Li, X.Y., et al., 2008. Microbial population dynamics during aerobic sludge granulation at different organic loading rates. *Water Research*, **42**(13):3552-3560.
<http://dx.doi.org/10.1016/j.watres.2008.05.005>
- Li, J., Xi, D.L., Shi, Y., 2008. Resistance distribution and fouling mechanism of dynamic membrane in wastewater treatment. *Journal of Chemical Industry and Engineering*, **59**(9):2309-2315 (in Chinese).
- Li, P., Wang, Y.X., Wang, Y.H., et al., 2010. Bacterial community structure and diversity during establishment of an anaerobic bioreactor to treat swine wastewater. *Water Science and Technology*, **61**(1):243-252.
<http://dx.doi.org/10.2166/wst.2010.807>
- Li, R., Huang, X., Wang, Z.Q., 2000. Hydraulic characteristics in a submerged membrane bioreactor. *Environmental Science*, **21**(5):47-50 (in Chinese).
- Liaw, R.B., Cheng, M.P., Wu, M.C., et al., 2010. Use of metagenomic approaches to isolate lipolytic genes from activated sludge. *Bioresource Technology*, **101**(21):8323-8329.
<http://dx.doi.org/10.1016/j.biortech.2010.05.091>
- Mannina, G., Cosenza, A., 2013. The fouling phenomenon in membrane bioreactors: assessment of different strategies for energy saving. *Journal of Membrane Science*, **444**:332-344.
<http://dx.doi.org/10.1016/j.memsci.2013.05.047>
- Mannina, G., Cosenza, A., Di Trapani, D., et al., 2016a. Membrane bioreactors for treatment of saline wastewater contaminated by hydrocarbons (diesel fuel): an experimental pilot plant case study. *Chemical Engineering Journal*, **291**:269-278.
<http://dx.doi.org/10.1016/j.cej.2016.01.107>
- Mannina, G., Capodici, M., Cosenza, A., et al., 2016b. Sequential batch membrane bio-reactor for wastewater treatment: the effect of increased salinity. *Bioresource Technology*, **209**:205-212.
<http://dx.doi.org/10.1016/j.biortech.2016.02.122>
- Meng, F.G., Zhang, H.M., Yang, F.L., et al., 2007. Characterization of cake layer in submerged membrane bioreactor. *Environmental Science and Technology*, **41**(11):4065-4070.
<http://dx.doi.org/10.1021/es062208b>
- Meng, F.G., Chae, S.R., Drews, A., et al., 2009. Recent advances in membrane bioreactors (MBRs): membrane fouling and membrane material. *Water Research*, **43**(6):1489-1512.
<http://dx.doi.org/10.1016/j.watres.2008.12.044>
- MOTIMO, 2006. User's Guide for Membrane Using. Tianjin MOTIMO Membrane Technology Co. Ltd., Tianjin, China (in Chinese).
- Muyzer, G., DeWaal, E.C., Uitterlinden, A.G., 1993. Profiling of complex microbial populations by denaturing gradient gel electrophoresis analysis of polymerase chain reaction-amplified genes coding for 16S rRNA. *Applied and Environmental Microbiology*, **59**(3):695-700.
- Pontoni, L., D'Alessandro, G., d'Antonio, G., et al., 2015. Effect of anaerobic digestion on rheological parameters and dewaterability of aerobic sludges from MBR and conventional activated sludge plants. *Chemical Engineering Transactions*, **43**:2311-2316.
<http://dx.doi.org/10.3303/CET1543386>
- Reboleiro-Rivas, P., Martín-Pascual, J., Morillo, J.A., et al., 2016. Interlinkages between bacterial populations dynamics and the operational parameters in a moving bed membrane bioreactor treating urban sewage. *Water Research*, **88**:796-807.
<http://dx.doi.org/10.1016/j.watres.2015.10.059>
- Rotaru, C., Woodard, T.L., Choi, S., et al., 2012. Spatial heterogeneity of bacterial communities in sediments from an infiltration basin receiving highway runoff. *Microbial Ecology*, **64**(2):461-473.
<http://dx.doi.org/10.1007/s00248-012-0026-x>
- Rudd, T., Sterritt, R.M., Lester, J.N., 1984. Complexation of heavy metals by extracellular polymers in the activated sludge process. *Journal of Water Pollution Control Federation*, **56**:1260-1268.
- Sanguinetti, C.J., Dias Neto, E., Simpson, A.J., 1994. Rapid silver staining and recovery of PCR products separated on polyacrylamide gels. *Biotechniques*, **17**(5):914-921.
- Silva, C.C., Viero, A.F., Andreote, F.D., et al., 2010. Monitoring the bacterial community dynamics in a petroleum refinery wastewater membrane bioreactor fed with a high phenolic load. *Journal of Microbiology and Biotechnology*, **20**(1):21-29.
- Tan, M., Qiu, G.L., Ting, Y.P., 2015. Effects of ZnO nanoparticles on wastewater treatment and their removal behavior in a membrane bioreactor. *Bioresource Technology*, **185**:125-133.
<http://dx.doi.org/10.1016/j.biortech.2015.02.094>
- Tu, T., Li, L., Mao, G.N., et al., 2012. Analysis of bacterial diversity in the Songhua River based on nested PCR and DGGE. *Acta Ecologica Sinica*, **32**(11):3505-3515 (in Chinese).
<http://dx.doi.org/10.5846/stxb201105160635>
- Wang, J.F., Wang, X., Zhao, Z.G., et al., 2008. Organics and nitrogen removal and sludge stability in aerobic granular sludge membrane bioreactor. *Applied Microbiology and Biotechnology*, **79**(4):679-685.
<http://dx.doi.org/10.1007/s00253-008-1466-6>
- Wang, X., Zhang, B., Shen, Z.Q., et al., 2010. The EPS characteristics of sludge in an aerobic granule membrane bioreactor. *Bioresource Technology*, **101**(21):8046-8050.
<http://dx.doi.org/10.1016/j.biortech.2010.05.074>
- Wei, Y.J., Ji, M., Li, G.Y., et al., 2012. Microbial and hydrodynamic properties of aerobic granules in a sequencing batch reactor treating landfill leachate. *Journal of Zhejiang University-SCIENCE A (Applied Physics & Engineering)*, **13**(3):219-229.

- <http://dx.doi.org/10.1631/jzus.A1100153>
- Xia, S.Q., Li, J.X., He, S.Y., et al., 2010. The effect of organic loading on bacterial community composition of membrane biofilms in a submerged polyvinyl chloride membrane bioreactor. *Bioresource Technology*, **101**(17):6601-6609.
<http://dx.doi.org/10.1016/j.biortech.2010.03.082>
- Ying, W., Yang, F., Bick, A., et al., 2010. Extracellular polymeric substances (EPS) in a hybrid growth membrane bioreactor (HG-MBR): viscoelastic and adherence characteristics. *Environmental Science and Technology*, **44**(22):8636-8643.
<http://dx.doi.org/10.1021/es102309y>
- Zhang, B., Sun, B.S., Ji, M., et al., 2008a. Analysis and succession of microbial community structure in a membrane bioreactor. *Acta Scientiae Circumstantiae*, **28**(11):2192-2199 (in Chinese).
- Zhang, B., Sun, B.S., Jin, M., et al., 2008b. Extraction and analysis of extracellular polymeric substances in membrane fouling in submerged MBR. *Desalination*, **227**(1-3):286-294.
<http://dx.doi.org/10.1016/j.desal.2007.06.032>
- Zhang, B., Sun, B.S., Ji, M., et al., 2010. Quantification and comparison of ammonia-oxidizing bacterial communities in MBRs treating various types of wastewater. *Bioresource Technology*, **101**(9):3054-3059.
<http://dx.doi.org/10.1016/j.biortech.2009.12.048>
- Zhang, Z.J., 2000. Wastewater Engineering, 2nd Edition. China Construction Industry Press, Beijing, China, p.386-387 (in Chinese).
- Ziembinska, A., Ciesielski, S., Gnida, A., et al., 2012. Comparison of ammonia-oxidizing bacterial community structure in membrane-assisted bioreactors using PCR-DGGE and FISH. *Journal of Microbiology and Biotechnology*, **22**(8):1035-1043.
<http://dx.doi.org/10.4014/jmb.1201.01014>

中文概要

题目: 膜生物反应器处理港口含油废水的膜污染行为及群落结构演变研究

目的: 采用膜生物反应器处理港口含油废水。考察运行

过程中膜污染行为特征, 分析引起膜污染的关键影响因素, 研究减弱膜污染的途径与方法; 考察反应器内群落结构演变, 分离鉴定优势菌种, 揭示运行条件和进水水质等宏观环境与微生物环境之间的对应关系。

创新点: 1. 分析出膜表面累积的胞外蛋白是膜污染严重和过膜压力增大的关键诱因; 2. 基于 Yusuf Chisti 和 Murray Moo Young 提出的气提液体上升流速模型, 结合胞外蛋白变化趋势, 提出降低过膜压力上升速度和缓解膜污染进程的有效措施; 3. 针对处理港口含油废水的生物系统进行种群结构研究及优势菌属的分离与鉴定。

方法: 1. 借助环境扫描电子显微镜 (SEM)、能量色散 X 射线光谱仪 (EDX) 和傅里叶红外光谱仪 (FTIR) 等分析手段表征膜污染物的主要成分; 2. 基于 Yusuf Chisti 和 Murray Moo Young 提出的气提液体上升流速模型, 提出缓解膜污染进程的措施, 并验证所提措施的有效性 (图 3 和 9); 3. 通过巢式 PCR-DGGE 技术对处理港口含油废水的膜生物反应器不同运行阶段的微生物群落结构进行研究, 并采用克隆技术对优势微生物进行菌种鉴定 (图 10 和表 3)。

结论: 1. 采用一体化厌氧/好氧-膜生物反应器来处理港口含油废水的优点是对有机污染物和油类等污染物的去除效率高, 但在其运行过程中膜污染严重。2. 分析发现胞外聚合物是引起膜污染物的主要因素 (图 3~6); 组分分析进一步表明膜表面累积的胞外蛋白是膜污染严重和过膜压力增大的关键诱因 (图 7~9)。3. 通过增大反应器曝气量, 调整反应器结构参数可有效降低过膜压力上升速度, 缓解膜污染进程。4. 反应器内细菌群落结构平稳。5. 克隆测序结果表明: 膜生物反应器内从毛单胞菌属在低曝气环境下繁殖能力强, 且可能是引起膜污染的特征微生物; 红环菌科细菌更适应高曝气条件, 是降解含有油类污染物的特征细菌。

关键词: 膜污染; 胞外聚合物; 港口含油废水; 群落结构